Tellus (1983), *35B*, 81–91

Overlapping effect of atmospheric H_2O, CO_2 and O_3 on the CO_2 radiative effect

By WEI-CHYUNG WANG and P. BARRY RYAN, *Atmospheric and Environmental Research, Inc., 840 Memorial Drive, Cambridge, Massachusetts 02139, U.S.A.*

(Manuscript received August 24, 1981; in final form August 2, 1982)

ABSTRACT

The effect of overlapping of atmospheric H_2O, CO_2 and O_3 absorption bands on the radiation budget perturbation caused by CO_2 doubling is investigated. Since the effect depends on the amount of gases in the atmosphere as well as on the strength of the absorption bands, we examine the effect associated with the variation of gas abundance using a narrow band representation for the absorption bands. This band representation allows for the absorption band structure and thus accounts for the correlation of the spectral feature of the absorbing gases.

It is found that the presence of H_2O and O_3 has a relatively small influence on the CO_2-induced perturbation of both solar and thermal radiation in the stratosphere. However, in troposphere and surface, the overlapping effect appears to be quite significant and changes the vertical distribution of the CO_2-induced radiation energy perturbation. For example, in the infrared, the effect is to reduce the effectiveness for CO_2 to emit and in the mean time increases the tropospheric absorption of downward thermal flux from the stratosphere due to CO_2 increase; the net effect of the overlapping of gases is to increase the tropospheric warming and decrease the surface warming caused by CO_2 increase. It is also found that the overlapping effect exhibits strong seasonal and latitudinal variations due primarily to variations in atmospheric H_2O.

1. Introduction

Increases in the atmospheric CO_2 concentration, due largely to fossil fuels utilization (cf. DOE, 1980; CEQ, 1981) are believed to cause radiative cooling in the stratosphere and warming in the troposphere and surface with subsequent effect on the earth's climate (NAS, 1979; Manabe and Stouffer, 1980; Hansen et al., 1981). Recent studies (Boughner, 1978; Penner and Luther, 1981; Callis and Natarajan, 1981) have further indicated that the CO_2-induced stratospheric cooling may also perturb the stratospheric O_3, which in turn could influence the biological activities as well as the climate (cf. *Stratospheric Ozone and Man*, 1982).

Since the CO_2-induced climatic changes are first initiated by the change of radiative forcing in the atmosphere through primarily the change of CO_2 greenhouse effect, an investigation of the uncertainties associated with the computed CO_2 radiative effect is therefore important to the overall CO_2-climate research program (DOE, 1980). One of the possible uncertainties may be related to the nature of overlapping of atmospheric H_2O, CO_2 and O_3 absorption bands (Elsasser, 1942; Goody, 1964; Ohring and Joseph, 1978; Ackerman, 1979).

It is known that atmospheric CO_2 has three major infrared absorption bands located at 667, 962 and 1064 cm^{-1} where atmospheric H_2O and O_3 also have absorption bands (cf. McClatchey et al., 1973; see Fig. 1). Consequently, the calculated CO_2 thermal radiative effect can be affected by the overlapping with H_2O and O_3. In addition, H_2O and CO_2 overlap in the near infrared, which can also affect solar radiation calculations.

The effect of overlapping of gases on the radiation calculations depends on both the *strength of the absorption bands* and the *amount of gases in the atmosphere* (cf. Elsasser, 1942; Goody, 1964).

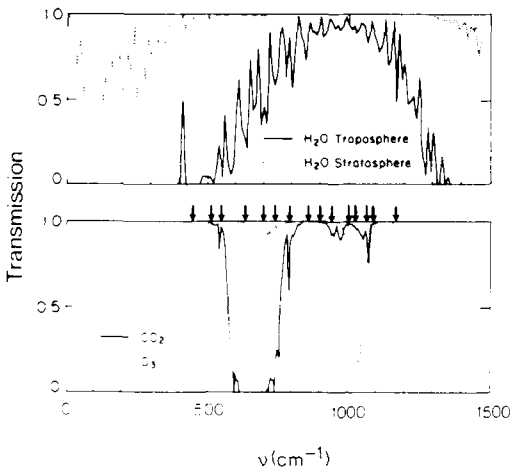

Fig. 1. Transmission of thermal radiation by atmospheric gases for present-day abundance (after Wang et al., 1976). Water vapor continuum, which is not shown is believed to be important in the 800–1200 cm^{-1} window region. The arrows indicate the band width of the several narrow bands. The band model parameters are obtained based on the least square fitting of the McClatchey et al. (1973) line-by-line calculated transmissions (cf. Appendix).

Consequently, there are possibly two sources of uncertainties in the computed CO_2 radiative effect related to overlapping with H_2O and O_3.

Firstly, the amount of atmospheric gases, such as H_2O and O_3 varies greatly in space and time; for example, the column amount of atmospheric H_2O can decrease by a factor of ten going from equator to poles. Consequently, the calculated CO_2 radiative effect may depend on latitudes and seasons (see Ramanathan et al., 1979; Newell and Dopplick, 1979; Fels et al., 1980). Ackerman (1979) has used high spectral resolution to evaluate the transmission functions in the 15 μm CO_2 band regime. The results indicate that it is important to treat the overlap region correctly especially when computing variations due to changing CO_2 concentrations.

Secondly, the overlapping of absorption bands is generally treated in climate models by employing the multiplication law (cf. Elsasser, 1942), i.e., the total transmission of a mixture of gases is equal to the product of the individual gas transmission. Strictly speaking, the multiplication law holds only if zero correlation exists between spectral features of overlapping gases. The treatment is found to be reasonably accurate for finite but small spectral intervals, the *narrow band representation* (Goody, 1964). However, when the spectral interval covers the total absorption band, the *wide band representation* (GARP, 1975, 1978), with band width of the order of a few hundred wave numbers, the treatment which is equivalent to assuming grey absorption (cf. Tien, 1968), thus ignoring the correlation between spectral features of overlapping gases, may potentially introduce errors.

In addition, the absorption bands of the gases may not necessarily have the same total band width; for example, the 667 cm^{-1} CO_2 band is much wider than the 714 cm^{-1} O_3 band (see Fig. 1). Consequently, proper consideration of the overlapping effect between the absorption bands would require a subdivision of the 667 cm^{-1} CO_2 band into at least three spectral intervals, which may not be acceptable to climate models since the computational time is directly proportional to the number of spectral intervals used.

In this paper, we aim at investigating the first uncertainty and intend to estimate through sensitivity study, the overlapping effect of atmospheric H_2O, O_3 and CO_2 on the radiative perturbation due to a factor of two increase in present atmospheric CO_2 abundance of 330 ppmv. We shall examine, separately, the effect on perturbation of radiative heating/cooling in stratosphere, troposphere and ground due to such CO_2 increase. The calculations are based on narrow band representation such that the correlation of the spectral feature of the absorbing gases can be adequately accounted for. In a separate paper, we will examine the overlapping effect in the wide band representation. In particular, comparisons will be made between the narrow and the wide band representations.

2. Narrow band treatment in radiation model

The CO_2 sensitivity studies were performed using the radiation model developed earlier at Goddard Institute for Space Studies/NASA (cf. Wang et al., 1976, 1981a, b; Lacis et al., 1979). In the model, the solar radiation is calculated based on Lacis and Hansen (1974), except that the frequency integration scheme described in Lacis et al. (1979) is used to calculate the total solar flux. Since we did not describe the detail of thermal radiation cal-

culations in those studies, an appendix is provided to explain the method.

In the narrow band representation, the 15 μm CO_2 spectral band regime (450–945 cm^{-1}) is divided into 8 variable width narrow spectral intervals and the 9.4 and 10.4 μm band regime (945–1160 cm^{-1}) into 5 intervals (see Fig. 1). The Malkmus (1967) narrow band model parameters associated with each spectral interval for the absorbing gases of H_2O, CO_2, O_3 and the continuum are generated from the basic data set described in Appendix 6.5. For an inhomogeneous atmosphere, ten probability values (see Appendix 6.3) were used to represent the non-gray nature of the molecular band structure inside each narrow spectral interval. Therefore, the total *effective* number used for frequency integration is 130 for the CO_2 band regimes.

3. Results

Sensitivity studies were conducted to examine the effect of overlapping of H_2O, CO_2 and O_3 on the CO_2 radiative effect. In the studies, we first calculate the CO_2 radiative heating/cooling of the unperturbed state (reference CO_2 abundance 330 ppmv) with and without H_2O and O_3 and then repeat the calculations for 660 ppmv CO_2.

Table 1 shows the calculated CO_2-induced energy perturbation in the stratosphere, troposphere and ground for the U.S. Standard (1976) atmospheric temperature and O_3 distribution, and the relative humidity profile of Manabe and Wetherald (1967). To further illustrate the overlapping effect, we have also shown in Table 1 the change of energy flux perturbation in the upward (U) and downward (D) directions.

Table 1. *Perturbation of radiative heating/cooling ($W\ m^{-2}$) in stratosphere (S), troposphere (T) and ground (G) due to a factor of two increase of CO_2 abundance (330 ppmv). The U.S. Standard (1976) atmospheric temperature and O_3 distribution and the relative humidity profile of Manabe and Wetherald (1967) are used*

		Solar			Thermal			Earth-atmosphere system
		S	T	G	S	T	G	
A. Clear atmosphere								
a. CO_2 only	U	0.00	0.03	0.13	−0.65	5.16	0	
	D	0.61	0.72	−1.32	−2.03	−7.34	9.37	
	N	0.61	0.74	−1.19	−2.67	−2.19	9.37	4.64
b. $H_2O + CO_2 + O_3$	U	0.00	0.02	0.06	−0.83	3.87	0	
	D	0.57	0.05	−0.62	−1.93	0.22	1.71	
	N	0.57	0.06	−0.56	−2.75	4.10	1.71	3.13
B. Three-cloud atmosphere ($H_2O + CO_2 + O_3$)								
	U	0.00	0.14	0.04	−0.80	3.04	0	
	D	0.57	−0.18	−0.40	−1.93	0.78	1.15	
	N	0.57	−0.04	−0.36	−2.73	3.82	1.15	2.41

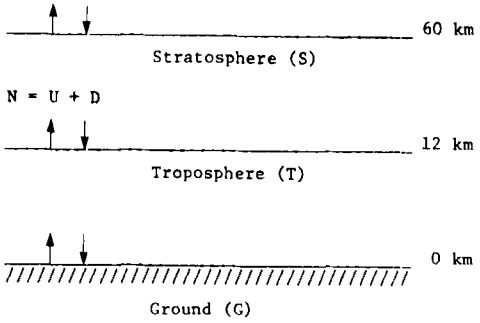

In a clear atmosphere with CO_2 only, absorption of solar radiation due to CO_2 doubling is increased by 0.61 and 0.74 Wm^{-2}, in the stratosphere and troposphere, respectively, while the ground is cooled by 1.19 Wm^{-2}. Most of the changes can be attributed to the changes of downward solar radiation, since the effect of absorption of upward (reflected) solar radiation is small; here the surface reflectivity is assumed to be 0.1.

On the other hand, perturbation of thermal radiation results in cooling of both the stratosphere and troposphere by 2.67 and 2.19 Wm^{-2}, respectively, with significant heating of the surface by 9.37 Wm^{-2}. The increased downward tropospheric thermal flux to the surface is mainly from the 15 μm CO_2 band wings (550–640 cm^{-1} and 740–800 cm^{-1}) while the contributions from the band peak regime (640–700 cm^{-1}) and the far wings (450–550 cm^{-1} and 800–900 cm^{-1}) are relatively small. It is also interesting to note that the 9.4 and 10.4 μm CO_2 bands contribute about 15% of the total surface warming. The tropospheric cooling of 7.34 Wm^{-2} in the downward direction is partially offset by the warming of 5.16 Wm^{-2} as a result of absorption of upward surface emission. The whole earth-atmosphere system is warmed by 4.64 Wm^{-2} for CO_2 doubling.

The effect of the presence of H_2O and O_3 is to increase the atmospheric opacity and thus to reduce the *effectiveness* of CO_2 as a radiative material. Consequently, for this particular case, it is found that a doubling of CO_2 abundance yields a 3.13 Wm^{-2} warming of the earth-atmosphere system, which is substantially smaller than that found for a pure CO_2 atmosphere. In addition, note that the distribution of the radiative heating/cooling perturbation for an H_2O, CO_2 and O_3 atmosphere is also very different, especially in the thermal infrared region. The surface warming is reduced to 1.71 Wm^{-2}, while the troposphere, instead of cooling, is actually warmed by 4.10 Wm^{-2}. This different tropospheric response is primarily a result of the small heating of 0.22 Wm^{-2} found in the downward direction, which is in contrast to 7.34 Wm^{-2} cooling for the case of CO_2 only. This happens because, as mentioned before, overlapping of H_2O, CO_2 and O_3 in the troposphere tends to reduce the effectiveness for CO_2 to emit and, in the meantime, increases the tropospheric absorption of downward flux from the stratosphere due to CO_2 doubling.

The distribution of the solar radiation perturbation in the troposphere and ground is also found changed, although the magnitude of the

Table 2. *Perturbation of thermal radiative heating/cooling (Wm^{-2}) in stratosphere (S), troposphere (T) and ground (G) due to a factor of two increase in CO_2 abundance (330 ppmv) for clear atmospheric models of McClatchey* et al. *(1972)*

		CO_2 only			$H_2O + CO_2 + O_3$		
		S	T	G	S	T	G
A. Subarctic winter	U	−0.09	2.47	0	−0.19	2.19	0
	D	−1.98	−3.94	5.92	−1.87	−0.85	2.72
	N	−2.07	−1.47	5.92	−2.06	1.34	2.72
B. Subarctic summer	U	−0.62	4.89	0	−0.79	3.09	0
	D	−2.47	−6.72	9.19	−2.35	0.90	1.44
	N	−3.09	−1.83	9.19	−3.14	3.99	1.44
C. Mid-latitude winter	U	−0.15	3.68	0	−0.29	2.85	0
	D	−2.06	−5.32	7.38	−1.96	−0.37	2.33
	N	−2.21	−1.64	7.38	−2.26	2.48	2.33
D. Mid-latitude summer	U	−0.52	5.66	0	−0.73	3.59	0
	D	−2.25	−8.04	10.29	−2.14	1.06	1.08
	N	−2.77	−2.37	10.29	−2.87	4.66	1.08
E. Tropics	U	−0.24	6.31	0	−0.44	3.67	0
	D	−2.16	−8.98	11.14	−2.09	1.30	0.78
	N	−2.40	−2.67	11.14	−2.53	4.97	0.78

change is much smaller. For this atmospheric model, the overlapping effect has a relatively small influence on the perturbation of both the solar and thermal radiation in the stratosphere.

We have also examined the overlapping effect when three cloud layers are present (see Wang et al., 1981a; cf. Appendix). Again, the presence of clouds has a small effect on the CO_2-induced energy perturbation in the stratosphere in both the solar and thermal regimes. However, as one may expect, the distribution of solar and thermal energy perturbation in the troposphere and the ground is different from that found in a clear atmosphere. For this case the earth-atmosphere system is warmed by 2.41 Wm^{-2}.

The troposphere-surface system is warmed by 4.57 Wm^{-2}, a value comparable to the hemispheric annual mean value of 4.12 Wm^{-2} as calculated from a zonally-averaged seasonal model (Ramanathan et al., 1979). Note that the effect of perturbation of solar radiation in the stratosphere and ground due to CO_2 doubling is a negative feedback effect and tends to reduce the thermal effect by ~20% in the stratosphere and ~30% in the ground.

Previous analyses are based on the use of a global averaged model atmosphere. For comparison purposes, we have also investigated the overlapping effect at different latitudes and seasons. Table 2 shows the CO_2-induced perturbation of thermal radiative heating/cooling with and without H_2O and O_3 for the five model atmospheres of McClatchey et al. (1972).

The differences between the CO_2 and the H_2O + CO_2 + O_3 atmospheres for all five models are found to be qualitatively similar to the global average model. In the stratosphere, the effect of addition of H_2O and O_3 is to increase slightly the CO_2-induced radiative cooling resulting from the partial compensation between the changes in the upward and downward directions. Similar tropospheric response, i.e., changing from cooling to heating, is observed, primarily caused by the large change in the downward direction. It is therefore quite clear the H_2O plays a major role in affecting the CO_2 radiative effect.

It is also found that in the stratosphere, the differences among the models are relatively small, and can be attributed (as can be seen from the CO_2 only case) primarily to the differences in the temperature distribution. On the other hand, tropospheric heating/cooling in the downward direction is found to be different, depending on the cancellation between the increase of warming due to absorption of downward flux from stratosphere and cooling due to emission from troposphere to ground. It is therefore concluded that the overlapping effect has different influence at different latitudes and seasons.

Comparison of the present calculations with values obtained by Ramanathan et al. (1979) and Newell and Dopplick (1979) shows good agreement, although the present model yields larger tropospheric warming and smaller surface warming especially in the tropics (for example, see Fig. 8 of Ramanathan et al., 1979).

4. Conclusions

In the present study, we have investigated the overlapping effect of atmospheric H_2O, CO_2 and O_3 absorption bands on the radiation energy perturbation caused by increased CO_2 abundance. In particular, we investigate the thermal infrared regime because of the dominance of the greenhouse effect in the overall CO_2 radiative effect.

The results indicate that overlapping of CO_2 with H_2O and O_3 has a negligible effect on the calculated CO_2 radiative effect in the stratosphere but could have large influence in the troposphere and surface. Our results further suggest that the overlapping effect exhibits large seasonal and latitudinal variations due primarily to variations of H_2O. In addition, it is found that the effect of perturbation of solar radiation in the stratosphere and surface due to CO_2 increase cannot be ignored for CO_2 climate study. The effect is a negative feedback effect and could reduce the CO_2-induced perturbation of thermal radiation by about 20–30%.

Note, however, that the sensitivity study we performed is based on the narrow band representation. Due to the fact that the overlapping effect on the infrared flux at a given altitude depends on the changes in both the local emission and the transmitted flux reaching that level, and thus clearly is a strong function of wavelength, a more detailed spectral integration scheme such as the line-by-line calculation may potentially further yield a different calculated CO_2 radiative effect. Because of the extreme importance of the cal-

culated CO_2 radiative effect for the overall CO_2 climate studies, continued work on further quantifying and eventually reducing its uncertainty should be actively pursued.

5. Acknowledgement

This study was supported jointly by the Federal Aviation Administration under contract #DTFA01-80-C10101, the Chemical Manufacturers Association under contract #FC80-311 and the Department of Energy under contract #DE-AC02-81ER 60023. We are indebted to an anonymous reviewer for several suggestions which have clarified the presentation.

6. Appendix. Thermal radiation model used in CO_2 climate sensitivity studies

In this Appendix we present the thermal spectral flux formulation, the correlated k-distribution method for frequency integration in an inhomogeneous atmosphere, the consideration of overlapping of gases and the spectral absorption data used in narrow band radiation calculations.

6.1. *Thermal spectral flux formulation*

For a homogeneous clear layer (i.e., no aerosol or cloud particles) with assumed linear Planck intensity distribution (see Fig. A1), the spectral intensities $I^{\uparrow}$ and $I^{\downarrow}$ emitted from the top and bottom layer can be readily written in analytic form

$$\begin{cases} I^{\uparrow} = I_t - I_b t - \mu m(1-t) \\ I^{\downarrow} = I_b - I_t t + \mu m(1-t) \end{cases} \tag{A1}$$

where I_t and I_b are the spectral Planck intensities at the layer top and bottom respectively, and $\mu = \cos\theta$ with θ the zenith angle. Note that both $I^{\uparrow}$ and $I^{\downarrow}$ are associated with positive μ values. The spectral intensity transmission function t, the Planck intensity gradient m and the optical thickness τ are defined,

$$\begin{cases} t = e^{-\tau/\mu} \\ m = (I_t - I_b)/\tau \\ \tau = ku \end{cases} \tag{A2}$$

where k is the monochromatic absorption coefficient and u the gas amount.

Multiplying eq. (A1) by $2\pi\mu$ and integrating over μ from 0 to 1, we obtain the expressions for the spectral fluxes $E^{\uparrow}$ and $E^{\downarrow}$ emitted from the top and bottom layer,

$$\begin{cases} E^{\uparrow} = B_t(1-\bar{t}) - \dfrac{2\pi m}{3}(1 - e^{-\tau} - \tau\bar{t}) \\ E^{\downarrow} = B_b(1-\bar{t}) + \dfrac{2\pi m}{3}(1 - e^{-\tau} - \tau\bar{t}) \end{cases} \tag{A3}$$

where $B_t = \pi I_t$ and $B_b = \pi I_b$. The spectral flux transmission function $\bar{t} = 2E_3(\tau)$ and E_3 is the third exponential integral function.

The procedure for computing the thermal spectral flux in a multilayered atmosphere is similar to that used by Lacis and Hansen (1974), except that the emission terms must be carried along. In addition, it should be noted that if the *flux* formulation (eq. (A3)) is used, the flux transmission function through a number of layers (the product of transmissions for the individual layers) is a function of the sum of the optical paths,

$$\prod_l \bar{t}(\tau_l) = \bar{t}\left(\sum_l \tau_l\right) = 2E_3\left(\sum_l \tau_l\right).$$

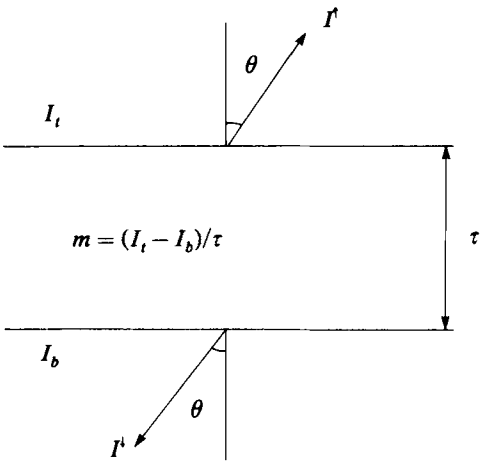

Fig. A1. Homogeneous layer emissions.

6.2. *Frequency integration*

To obtain the total thermal flux would require the integration of the spectral flux discussed above over the total spectral regime. In general, because of the complicated molecular absorption band structure of the trace gases, a rigorous frequency

integration would require a line-by-line integration which clearly is very time-consuming and not acceptable for use in climate models. Our approach to this problem is the application of the correlated k-distribution method (cf. Lacis et al., 1979).

Firstly, we discuss the use of the k-distribution method for a homogeneous layer. Dividing the total spectral regime into N *narrow* intervals $\Delta\nu_i$ so that inside each interval the Planck flux can be assumed constant, the total flux at the top layer, for example, can then be evaluated by

$$F^{\uparrow} = \int_0^{\infty} E^{\uparrow}\,\mathrm{d}\nu \simeq \sum_i^N \int_{\Delta\nu_i} E_i^{\uparrow}\,\mathrm{d}\nu. \tag{A4}$$

Using the absorption coefficient k as the variable of integration together with an appropriate kernel function (cf. Domoto, 1974), the frequency integration can be transformed to the form

$$\frac{1}{\Delta\nu}\int_{\Delta\nu} X(\nu)\,\mathrm{d}\nu = \int_0^{\infty} X(k)f(k)\,\mathrm{d}k = \int_0^1 X(k)\,\mathrm{d}g(k), \tag{A5}$$

where $f(k)$ is the inverse transmission function or k-distribution function and $g(k)$ is the cumulative k-distribution function. Specifically, in eq. (A4), $X = 2E_3(\tau)$ or $(1 - e^{-\tau})/\tau$.

In a homogeneous layer, the $f(k)$ is formerly related to the mean transmission function $T(u)$ (cf. Arking and Grossman, 1972; Domoto, 1974; Wiscombe and Evans, 1977),

$$T(u) \equiv \frac{1}{\Delta\nu}\int_{\Delta\nu} e^{-ku}\,\mathrm{d}\nu \equiv \int_0^{\infty} f(k)\,e^{-ku}\,\mathrm{d}k \equiv \int_0^1 e^{-ku}\,\mathrm{d}g(k). \tag{A6}$$

The $f(k)$ for a given gas at a specified $\Delta\nu$ is the probability density function such that $f(k)\,\mathrm{d}k$ is the fraction of the frequency interval for which the absorption coefficient is between k and $k + \mathrm{d}k$. Eq. (A6) reveals that the transmission depends on the distribution of k values within $\Delta\nu$, but not on the ordering of the values. As indicated in Arking and Grossman (1972), the lack of a simple expression of $f(k)$ for randomly distributed lines is a major drawback for this alternative way of performing frequency integration.

However, Domoto (1974) has shown that by choosing the Malkmus (1967) narrow band model

$$T(u) = \exp\left\{-\frac{\pi}{2}B\left[\left(1 + \frac{4Su}{\pi B}\right)^{1/2} - 1\right]\right\}, \tag{A7}$$

$f(k)$ as well as $g(k)$ can be expressed analytically

$$\begin{cases} f(k) = \dfrac{1}{2k^{3/2}}(SB)^{1/2}\exp\left[\dfrac{\pi B}{4}\left(2 - \dfrac{k}{S} - \dfrac{S}{k}\right)\right] \\ g(k) = \dfrac{1}{2}\left\{e^{\pi B}\,\mathrm{erfc}\left[\sqrt{\dfrac{\pi BS}{4k}} + \sqrt{\dfrac{\pi Bk}{4S}}\right]\right. \\ \qquad \left. + \mathrm{erfc}\left[\sqrt{\dfrac{\pi BS}{4k}} - \sqrt{\dfrac{\pi Bk}{4S}}\right]\right\} \end{cases} \tag{A8}$$

where S and B are the mean line intensity and line half-width, respectively, and erfc( ) is the complementary error function. Domoto and Wang (1974) have used the method to investigate the thermal radiative effect of clouds.

6.3. *Inhomogeneous atmosphere*

For an inhomogeneous atmosphere, the ordering information of k-values is important and therefore makes the direct use of the method very difficult (cf. Arking and Grossman, 1972). However, an approximate method, called the correlated k-distribution method, has been developed by Lacis et al. (1979). The method is based on the assumption that the k-distribution functions at all altitudes are simply correlated in frequency space, i.e., the strongest absorption occurs at the same frequencies at all altitudes and similarly for the weakest absorption. Eq. (A5) can therefore be approximated by integrating over M discrete Δg_j intervals, i.e.,

$$\frac{1}{\Delta\nu}\int_{\Delta\nu} X(\nu)\,\mathrm{d}\nu \simeq \sum_j^M X(k_j)\,\Delta g_j. \tag{A9}$$

To ensure that the total transmission in eq. (A6) is conserved, values of k_j are evaluated according to

$$e^{-k_j u}\,\Delta g_j = T_j(u) = \int_{g_j}^{g_{j+1}} e^{-ku}\,\mathrm{d}g. \tag{A10}$$

The integral in eq. (A10) can be obtained in analytic form with the use of eq. (A8). Consequently, the inhomogeneous effect is implicitly included through the pressure and temperature dependence of S and B values.

This maintenance of the same relative rank of absorption coefficients over the entire pressure range of the atmosphere is rigorously correct for a single spectral line and for a uniform Elsasser (1942) band model. For a real gaseous spectrum, it is expected that errors may occur, as a result of overlapping of absorption lines. However, the overall accuracy of the method is remarkable as demonstrated by comparing with line-by-line calculations for the 9.6 μm O_3 band (see Lacis et al., 1979). It is found that the correlated k-distribution method gives the O_3 heating rates within 0.1 K day^{-1} of line-by-line calculations while the commonly used pressure-scaling and Curtis-Godson approximations fail to yield accurate results (Walshaw and Rodgers, 1963).

6.4. *Overlapping gases*

For overlapping gases, we adopted the commonly-used multiplication law (cf. Elsasser, 1942). In this treatment, the total transmission $T_{\Delta\nu}$ averaged over a narrow spectral interval $\Delta\nu$ is assumed to be equal to the product of the individual gaseous transmission, T_l, i.e.

$$T_{\Delta\nu} = \prod_{l}^{L} T_l \qquad \text{(A11)}$$

where L is the number of gases. The use of the k-distribution method would therefore require $\prod_l^L M_l$ number of Δg intervals to carry out the frequency integration (see eq. (A9)), which is clearly unacceptable for climate studies. Therefore, we have adopted the following numerical procedure to account for the overlapping of gases.

For illustrative purpose, we will use two gases with the same set of Δg values. From eq. (A10), the $T_{1j}(u_1)$ and $T_{2j}(u_2)$ associated with Δg_j can be calculated. We then rearrange the composite transmission $T_{ik} = T_{1i} x T_{2k}$ associated with $\Delta g_i \Delta g_k$ in a monotonically decreasing order. Next, the cumulative composite transmission T_j associated with Δg_j is calculated by summing up the T_{ik} such that the sum of the associated $\Delta g_i \Delta g_k$ is equal to Δg_j. Finally, the values of τ_j to be used in eq. (A9) are calculated by

$$\tau_j = -\ln (T_j).$$

Note that for overlapping gases, τ_j, instead of k_j, is the fundamental parameter. We do not have any theoretical justification for this somewhat arbitrary treatment. It is strictly a matter of computational economy. However, the correlation between weak and strong absorptions between the two gases is somewhat considered. Furthermore and more importantly, the condition of eq. (A11) is rigorously enforced.

6.5. *Band model parameters*

To perform the radiation calculations, it is therefore necessary to obtain k_j values which in turn depend on the Malkmus model band parameters S and B. Here we describe the procedures for extracting the basic data set from the absorption line data.

In a given narrow spectral interval (~5 cm^{-1}), we use the tabulated absorption line coefficients for H_2O, CO_2, O_3 and other gases compiled by McClatchey et al. (1973) to compute the line-by-line absorptions over homogeneous paths at specified pressure and temperature. Overall, 12 pressure levels (1.0, 0.7, 0.5, 0.3, 0.1, 0.05, 0.01, 0.005, 0.002, 0.001, 0.0005, and 0.0001 atm.) and 3 temperatures (204, 250 and 296 K) were used to calculate the line-by-line absorption as a function of gas amount. Next, we obtain, for each gas, a table of S and B by least square fitting of the calculated line-by-line absorptions. The fitting accuracy for the narrow spectral intervals is typically within 1 to 2% over the above pressure–temperature range for the gas amount encountered in the present atmosphere. It is quite clear that the present approach for extracting the band model parameters is time-consuming and different from those used conventionally [for example, see Table 5.5 of Goody (1964) and Appendix 10 of Houghton (1977)]. However, for homogeneous conditions, the transmission values are identical to line-by-line calculations.

Note that the approach is not limited by the changing line shape with altitude; we can use the appropriate Voigt line profile for each altitude and obtain S and B parameters. In the thermal infrared, the "e-type" water vapor continuum in the 10 μm window regime (see Roberts et al., 1976) is also included.

The same procedures were applied to obtain the near infrared H_2O and CO_2 narrow band parameters based also on the McClatchey et al. absorption line data.

Table A1. *Comparison of computed 15 μm CO_2 band absorption with measurements*

P (mb)	T (K)	u (10^{20} molecules/cm^2)	Band absorption (cm^{-1})	
			Measurement* Ae	Calculation† Ac
1013.49	310	14.86	150.9	153.9
505.73		14.81	141.7	142.6
506.41		7.426	125.1	124.5
253.54		7.425	114.8	113.4
		3.718	97.1	95.2
126.771		3.712	84.3	80.9
		1.859	64.5	64.0
63.36		3.851	72.7	68.3
		1.856	54.5	52.2
31.65		3.563	60.5	55.6
		1.925	43.6	43.8
15.76		1.774	35.6	33.3
1000.90	247	37.22	151.2	145.1
507.08	244	18.87	125.3	117.5
253.54		9.433	102.0	92.9
126.77		4.717	77.0	65.7
63.38	245	2.349	51.1	41.6
31.69		1.174	30.7	25.2
15.78		0.5847	17.0	14.0
7.96	246	0.2936	9.3	7.7

* Gryvnak et al. (1976); the band width is 560–780 cm^{-1}.
† The band width is 550–800 cm^{-1}.

Since the uncertainty of the calculated CO_2 radiative effect is also related directly to the CO_2 absorption data, we have therefore compared the 15 μm CO_2 band absorption used in the radiation model with available measurements. Table A1 shows the comparisons between the calculated and the measured total band absorption for several pressures and temperatures.

It can be seen that there is good agreement between the measured and the calculated values, with the latter generally being smaller. At low pressure regions, however, the discrepancy becomes somewhat larger. One possible uncertainty may be related to the interpolation of the band model parameters with respect to pressures and temperatures, which differ from those used in the laboratory measurements. On the other hand, the differences may be also related to the uncertainties associated with the absorption line parameters (Drayson, 1966; Goldman and Kyle, 1968; McClatchey and Rothman, personal communication, 1981). Nevertheless, the difference is comparable to the measurement uncertainties especially at low pressures and temperatures, as discussed by Gryvnak et al. (1976).

Ultimately all calculations must be validated by comparison with observations, such as the one performed by Ellingson and Gille (1978).

6.6. *Cloudy atmosphere*

In the present study, we primarily investigate the overlapping effect in a clear atmosphere. However, for illustrative purposes, the effect is also examined in the presence of layer clouds (Table 1). To calculate the thermal radiation in the presence of cloud particles, we have adopted a parameterized form of the two-stream approximation. Values of the coefficients in the parameterization are obtained based on computations with the doubling and adding method. Similarity relations (van de Hulst and Grossman, 1968) were then used to scale the scattering optical thickness and single scattering albedo for clouds to values appropriate for isotropic scattering, which is an adequate approximation because of the simple dependence of thermal radiation on zenith angle.

REFERENCES

Ackerman, T. P. 1979. On the effect of CO_2 on atmospheric heating rates. *Tellus 31*, 115–123.

Arking, A. and Grossman, K. 1972. The influence of line shape and band structure on temperatures in planetary atmospheres. *J. Atmos. Sci. 29*, 937–949.

Boughner, R. E. 1978. The effect of increased carbon dioxide on stratospheric ozone. *J. Geophys. Res. 83*, 1326–1332.

Callis, L. B. and Natarajan, M. 1981. Atmospheric carbon dioxide and chlorofluoromethanes: combined effects on stratospheric ozone, temperature, and surface temperature. *Geophys. Res. Lett. 8*, 587–590.

Council on Environmental Quality. 1981. *Global energy futures and the carbon dioxide problem*, Executive Office of the President, Washington, D.C.

DOE. 1980. Carbon dioxide effects: research and assessment program. Report No. EV-0094. Dept. of Energy, Washington, D.C.

Domoto, G. A. 1974. Frequency integration for radiative transfer problems involving homogeneous non-gray gases: The inverse transmission function. *J. Quant. Spectroc. Radiat. Transfer 14*, 935–942.

Domoto, G. A. and Wang, W. C. 1974. Radiative transfer in homogeneous non-gray gases with non-isotropic particle scattering. *J. Heat Transfer, ASME Trans.*, August, 385–390.

Drayson, S. R. 1966. Atmospheric transmission in the CO_2 bands between 12 and 18 μm. *Appl. Opt. 5*, 385–391.

Ellingson, R. G. and Gille, J. C. 1978. An infrared radiative transfer model. Part 1: Model description and comparison of observations with calculations. *J. Atmos. Sci. 35*, 523–545.

Elsasser, W. M. 1942. Heat transfer by infrared radiation in the atmosphere. *Harvard Meteor. Stud. No. 6*, 107 pp.

Fels, S. B., Mahlman, J. D., Schwarzkopf, M. D. and Sinclair, R. W. 1980. Stratospheric sensitivity to perturbations in ozone and carbon dioxide: radiative and dynamical responses. *J. Atmos. Sci. 37*, 2265–2297.

GARP. 1975. JOC study conference on the physical basis of climate and climate modeling, Pub. No. 16.

GARP. 1978. JOC study conference on parameterization of extended cloudiness and radiation for climate models. GARP Climate Dynamics Sub-Programme.

Goldman, A. and Kyle, T. G. 1968. A comparison between statistical models and line-by-line calculation with application to the 9.6 μm ozone and 2.7 μm water vapor bands. *Appl. Opt. 7*, 1167–1176.

Goody, R. M. 1964. *Atmospheric Radiation: I. Theoretical Basis*. Oxford University Press, 436 pp.

Gryvnak, D. A., Burch, D. E., Alt, R. L. and Zgonc, D. K. 1976. Infrared absorption by CH_4, H_2O and CO_2. AFGL-TR-76-0246.

Hansen, J., Johnson, D., Lacis, A., Lebedeff, S., Lee, P., Rind, D. and Russell, G. 1981. Climate impact of increasing atmospheric carbon dioxide. *Science 213*, 957–966.

Houghton, J. T. 1977. *The physics of atmospheres*. Cambridge University Press, 203 pp.

Lacis, A. A. and Hansen, J. E. 1974. A parameterization for the absorption of solar radiation in the earth's atmosphere. *J. Atmos. Sci. 31*, 118–133.

Lacis, A. A., Wang, W. C. and Hansen, J. E. 1979. Correlated k-distribution method for radiative transfer in climate models: application to effect of cirrus clouds on climate. NASA CP-2029, E. R. Kreing (ed.), 416 pp.

Malkmus, W. 1967. Random Lorenz band model with exponential-tailed S^{-1} line-intensity distribution function. *J. Opt. Soc. Amer. 51*, 323–329.

Manabe, S. and Stouffer, R. J. 1980. Sensitivity of a global climate model to an increase of CO_2 concentration in the atmosphere. *J. Geophys. Res. 85*, 5529–5554.

McClatchey, R. A., Fenn, R. W., Selby, J. E. A., Volz, R. E. and Goring, J. S. 1972. Optical properties of the atmosphere. *Environ. Res. Paper No. 411*, AFCRL, 108 pp.

McClatchey, R. A., Benedict, W. S., Clough, S. A., Burch, D. E., Calfee, R. F., Fox, K., Rothman, L. S. and Goring, J. S. 1973. AFCRL atmospheric absorption line parameter compilation. *Environ. Res. Paper No. 434*, AFCRL, 78 pp.

NAS. 1979. Carbon dioxide and climate: a scientific assessment. National Climate Board, National Academy of Sciences: Washington, D.C.

Newell, R. E. and Dopplick, T. G. 1979. Questions concerning the possible influence of anthropogenic CO_2 on atmospheric temperature. *J. Appl. Meteor. 18*, 822–825.

Ohring, G. and Joseph, J. H. 1978. On the combined infrared cooling of two absorbing gases in the same spectral region. *J. Atmos. Sci. 35*, 317–322.

Penner, J. E. and Luther, F. M. 1981. Effects of temperature feedback and hydrostatic adjustment in a stratospheric model. *J. Atmos. Sci. 38*, 446–452.

Ramanathan, V., Lian, M. S. and Cess, R. D. 1979. Increased atmospheric CO_2: zonal and seasonal estimates of the effect on the radiation energy balance and surface temperature. *J. Geophys. Res. 84*, 4949–4958.

Roberts, R. E., Selby, J. E. A. and Biberman, L. M. 1976. Infrared continuum absorption by atmospheric water vapor in the 8–12 μm window. *Appl. Opt. 15*, 2085–2090.

Stratospheric Ozone and Man. 1982. Bower, F. A. and Ward, R. B. (eds.): CRC Press.

Tien, C. L. 1968. Thermal radiation properties of gases, *Advances in Heat Transfer 5*, 253–324.

U.S. Standard Atmosphere. 1976. U.S. Government Printing Office, Washington, D.C.

Van de Hulst, H. C. and Grossman, K. 1968. In *Atmospheres of Venus and Mars* (eds. J. C. Brandt and M. B. McElroy). New York: Gordon and Breach.

Wang, W. C., Sze, N. D., Ko, M. K. W. and Ryan, P. B. 1981a. Coupled effects of atmospheric N_2O, CH_4, CEMs and O_3 on the earth's climate. *Proceedings of the Quadrennial International Ozone Symposium*, Boulder.

Wang, W. C., Yung, Y. L., Lacis, A. A., Mo, T. and Hansen, J. E. 1976. Greenhouse effects due to man-made perturbations of trace gases. *Science 194*, 685–690.

Wang, W. C., Rossow, W. B., Yao, M. S. and Wolfson, M. 1981b. Climate sensitivity of a one-dimensional radiative-convective model with cloud feedback. *J. Atmos. Sci. 38*, 1167–1178.

Walshaw, C. D. and Rodgers, C. D. 1963. The effect of the Curtis-Godson approximation on the accuracy of radiative heating rate calculations. *Quart. J. Roy. Meteorol. Soc. 89*, 122–130.

Wiscombe, W. J. and Evans, J. W. 1977. Exponential-sum fitting of radiative transmission functions. *J. Comput. Phys. 24*, 416–444.